Published in IET Radar, Sonar and Navigation
Received on 1st December 2007
Revised on 8th July 2008
doi: 10.1049/iet-rsn:20080108

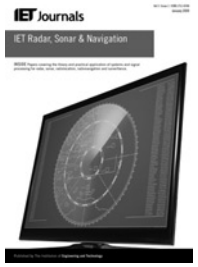

ISSN 1751-8784

Two-dimensional pulse-to-pulse canceller of ground clutter in airborne radar

X.-M. Li[1] *D.-Z. Feng*[1] *H.-W. Liu*[1] *M.-D. Xing*[1] *D. Luo*[2]

[1]*National Laboratory for Radar Signal Processing, Xidian University, Xi'an 710071, People's Republic of China*
[2]*Radar and Avionics Institute of AIVC, Wuxi 214063, People's Republic of China*
E-mail: xm_li@tom.com

Abstract: It is well known that in the airborne radar, the location of the ground clutter spectrum in the angle-Doppler space is dependent mainly on the platform velocity and radar parameters. The authors propose a two-dimensional pulse-to-pulse canceller (TDPC) that can make full use of such prior information. The more detailed formulations of the ground clutter model and the signal model are given in a matrix–vector form. The least-squares-typical cost function associated with the filter coefficient matrix of the TDPC is established on the basis of the ground clutter model and the signal model. Like the classical displaced phase centre antenna (DPCA) processing, the proposed TDPC is also a spatial-temporal suppressor of ground clutter and can decrease the ground clutter signals, even though the DPCA condition is not satisfied. The proposed TDPC can also be used as an efficient pre-filtering tool before the conventional moving target indication (MTI) processing and the classical adaptive processing. Moreover, if only the TDPC plus the conventional MTI is used, it takes less computational time than the adaptive canceller. Experimental results show that the proposed TDPC has the satisfactory ground clutter suppression capability by using both simulated data and measured data.

1 Introduction

In the airborne radar, ground clutter suppression is critical for moving target detection (MTD) since the ground clutter signals received by the airborne antenna array are strong and temporally and spatially coupled. Space-time adaptive processing (STAP) is an important technique for improving the detection performance of airborne radar systems [1–6]. By adaptively combining spatial and temporal samples, a significant increase in the output SCNR can be potentially achieved with the SCNR denoting the ratio of signal to clutter plus noise. Two main limitations of the application of STAP in practice include the high computational cost necessary for implementation and the large stationary sample support required for training the filter [2, 3]. These two limitations have motivated the development of suboptimal dimension-reduced STAP algorithms [2, 7–20]. The dimension-reduced STAP algorithms take low adaptive degrees of freedom (DOFs) and have low sampling requirements and low computational load so long as the clutter suppression performance is not compromised. Many dimension-reduced STAP algorithms have been proposed in the last decade or so. The displaced phase centre antenna (DPCA) [9] is one of the earliest techniques developed to address the issue of clutter mitigation in the space-time radar. This method performs clutter suppression via an echo-subtraction scheme. Klemm [2] proposed many dimension-reduced STAP algorithms in the space-time domain, the space domain only, the time domain only, or the space-time frequency domain. The factored approach (FA) [10, 11] and extended factored approach (EFA) [10, 12] are the Doppler transform-space adaptive processing. The joint domain localised [13, 14] algorithm was proposed on the basis of the idea of simultaneous reduction of DOFs in both space and time. The ΣΔ–STAP [15] approach reduces the spatial DOF to sum and difference beams only. Goldstein developed a dimension-reduced STAP based on a multistage Wiener filter [16]. The parametric adaptive matched filter [17] is implemented on the basis of approximating the interference spectrum with a multichannel autoregressive model of a low order. The non-homogeneity detector [18–20] can enhance clutter suppression performance and reduce the number of training data to obtain a good estimate of the covariance matrix. This is achieved by detecting and eliminating the outliers

from a large training set. These outliers are auxiliary samples that are statistically different.

In space-time processing of airborne radar signals, proper utilisation of prior information can certainly improve the MTD performance. In the knowledge-aided STAP [21–24] (KA-STAP), the digital terrain data were exploited to aid in choosing representative secondary data. The assumption is that the estimation of the covariance matrix will be improved by choosing secondary data whose terrain statistical characteristics are approximately stationary. Hence, STAP will cancel the terrain clutter more effectively. In addition, the knowledge-aided parametric covariance estimation STAP (KAPE-STAP) approach [25] exploits the knowledge to predict and estimate the clutter covariance matrix and pre-whiten the space-time clutter data. The stated objectives of these KA-STAP approaches are to reduce the covariance errors leading to detection performance loss and to improve the performance in complex and heterogeneous clutter environments. The nonlinear non-adaptive space-time clutter cancellation method [26] for the sidelooking airborne radar uses the constructed clutter covariance to generate the space-time clutter filter and makes the output of a bank of linear filters with pre-selected weights and variable spectral spread minimised. The clutter covariance matrix is constructed by using the knowledge of the pulse repetition frequency (PRF), platform velocity and channel spacing. The stated objectives of nonlinear non-adaptive space-time processing include the potential for reducing the computational load over certain STAP implementations and robustness in the presence of heterogeneous clutter. In the airborne radar, given the platform velocity and the radar parameters including the PRF, radar wavelength, configuration of the antenna array and so on, the location of the clutter spectrum in the angle-Doppler space is known in advance. For example, after transforming the space-time data to those in the angle-Doppler domain, the ground clutter spectra for the sidelooking airborne radar and non-sidelooking airborne radar are distributed along a line [2] and a family of declining elliptical curves [2], respectively, where the characteristics of the line and ellipses are determined by the platform velocity and radar parameters. This information can be useful prior information for clutter suppression in space-time processing.

This paper exploits the prior information and proposes a two-dimensional pulse-to-pulse canceller (TDPC) approach on the basis of the ground clutter model. The TDPC can effectively suppress the clutter not only for the sidelooking airborne radar but also for the non-sidelooking radar since the drift angle and elevation angle have been taken into account in the design of the TDPC. We expect the designed TDPC can filter out most of the ground clutter when the radar parameters are known and platform velocity is measured with high enough precision. Thus, like the well-known two-pulse or three-pulse ground clutter cancellers that have been used as typical temporal antiground clutter pre-filters in ground-based radar systems, the designed TDPC can be used as a spatial-temporal antiground clutter pre-filter in airborne radar systems so that MTD performance can be improved by the match of signals in both the spatial domain and Doppler domain. Moreover, the TDPC can also be used as a pre-filter before an adaptive algorithm. Since the TDPC eliminates most of the ground clutter before STAP, the STAP methods with the TDPC pre-filtering usually outperform the STAP approaches without the TDPC pre-filtering.

The rest of the paper is organised as follows. In Section 2, the ground clutter model and the target signal model are formulated in a matrix–vector form. The TDPC is given in Section 3. The TDPC is used as a pre-filter before the conventional moving target indication (MTI) and the FA in Section 4. In Section 5, performance of the TDPC is demonstrated via computer simulations for both the simulated and measured data. Conclusions are drawn in Section 6.

2 Ground clutter model and target signal model

To conveniently model the ground clutter and target signal in matrix–vector form, we assume the antenna mounted on an aircraft is a uniform linear array parallel to the ground. Let the place angle (or drift angle) between the array line and the flight velocity be marked φ_p. The array includes N directional sensors with spacing d between two adjacent elements. The radar transmits a coherent burst of K pulses during a coherent processing interval (CPI) at a constant PRF $f_r = 1/T$, where T is the pulse repetition interval (PRI). Thus, such a CPI lasts KT time units.

We assume that far-field conditions are satisfied, which means that the antenna size is very small compared with the range from radar to target. This implies that the antenna displacement caused by platform motion during a CPI, to the extent that it is taken into consideration for ground clutter suppression, is very small compared with the range. Let the velocity of the aircraft be V_a and the radar wavelength be λ, and then the kth ground clutter echo received by the nth sensor and arriving from a point scatter at the azimuth angle φ and elevation angle θ can be given by [2]

$$c_{nk}(\varphi) = a_k(\varphi)\exp\{j(2\pi/\lambda)[nd\cos\theta\cos\varphi + (2V_a/f_r)k\cos\theta\cos(\varphi+\varphi_p)]\} \quad (1)$$

where $n = 1, \ldots, N$ denotes the sensor index, $k = 1, \ldots, K$ indicates the slow time index and $a_k(\varphi)$ is the complex random amplitude.

With (1), the ground clutter echo scattered by all scatterers in a single range increment (bin) and received by the nth

doi: 10.1049/iet-rsn:20080108

sensor at the kth instant of time can be expressed as

$$x_{nk} = \int_0^{\pi} a_k(\varphi) \exp\left\{ j\frac{2\pi}{\lambda}\left[nd\cos\theta\cos\varphi + \frac{2V_a}{f_r}k\cos\theta\cos(\varphi+\varphi_p)\right]\right\} d\varphi + w_{nk} \quad (2)$$

where w_{nk} is the white noise received by the nth sensor at the slow time k. Let $\omega(\varphi) = \exp(j(2\pi/\lambda)(2V_a/f_r)\cos\theta\cos(\varphi+\varphi_p))$, $\omega_k(\varphi) = [\omega(\varphi)]^k$, and $z_n(\varphi) = \exp(j2\pi/\lambda nd\cos\theta\cos\varphi)$, and then (2) can be rewritten as

$$\begin{aligned} x_{nk} &= \int_0^{\pi} a_k(\varphi)\omega_k(\varphi)z_n(\varphi)d\varphi + w_{nk} \\ &= \int_0^{\pi} a_k(\varphi)[\omega(\varphi)]^k z_n(\varphi)d\varphi + w_{nk} \end{aligned} \quad (3)$$

If the ground clutter within one range bin is discretised into I small ground clutter patches along the azimuth angle φ, the discrete expression of (3) is described by

$$\begin{aligned} x_{nk} &= \sum_{i=1}^{I} z_n(\varphi_i)a_k(\varphi_i)\omega_k(\varphi_i) + w_{nk} \\ &= \sum_{i=1}^{I} z_n(\varphi_i)a_k(\varphi_i)[\omega(\varphi_i)]^k + w_{nk} \end{aligned} \quad (4)$$

where φ_i denotes the azimuth angle of the ith ground clutter patch.

Let $\boldsymbol{x}(k) = [x_{1k}, x_{2k}, \ldots, x_{Nk}]^T$ represent the kth ground clutter echo vector received by all the N sensors with superscript T denoting the transpose operation. Then, (4) can be further rewritten in matrix–vector form as

$$\boldsymbol{x}(k) = \boldsymbol{Z}\boldsymbol{B}(k)\boldsymbol{a}_k + \boldsymbol{w}(k) \quad (5)$$

where

$$\boldsymbol{Z} = \begin{pmatrix} z_1(\varphi_1) & \cdots & z_1(\varphi_I) \\ \vdots & \ddots & \vdots \\ z_N(\varphi_1) & \cdots & z_N(\varphi_I) \end{pmatrix} \quad (6a)$$

$$\boldsymbol{B}(k) = \mathrm{diag}(\omega_k(\varphi_1), \ldots, \omega_k(\varphi_I)) \quad (6b)$$

$$\boldsymbol{a}_k = [a_k(\varphi_1), \ldots, a_k(\varphi_I)]^T \quad (6c)$$

$$\boldsymbol{w}(k) = [w_{1k}, w_{2k}, \ldots, w_{Nk}]^T \quad (6d)$$

where $n = 1, \ldots, N$, $i = 1, \ldots, I$, and diag($\bullet$) is a diagonal matrix formed by the elements of its vector valued argument. It is seen that the matrix $\boldsymbol{Z}$ represents a spatial phase matrix, $\boldsymbol{B}(k)$ denotes the Doppler phase matrix, the vector $\boldsymbol{a}_k$ includes the random amplitude and phase vector, and $\boldsymbol{w}(k)$ represents the white noise vector received by the N sensors. Especially, let $\bar{\boldsymbol{B}} = \mathrm{diag}(\omega(\varphi_1), \ldots, \omega(\varphi_I))$, and then we have a relation $\boldsymbol{B}(k) = \mathrm{diag}([\omega(\varphi_1)]^k, \ldots, [\omega(\varphi_I)]^k) = [\mathrm{diag}(\omega(\varphi_1), \ldots, \omega(\varphi_I))]^k = \bar{\boldsymbol{B}}^k$, which shows that the temporal phase caused by the Doppler frequency changes linearly with the slow time.

It can be seen from (5) that the location of the clutter spectrum in the angle-Doppler space is determined by $\boldsymbol{Z}$ and $\boldsymbol{B}(k)$, where $\boldsymbol{Z}$ and $\boldsymbol{B}(k)$ depend only on φ, θ, V_a, λ and the array manifold. If the array manifold and λ are given in advance, and φ, θ and V_a can be measured or estimated with very high precision, then $\boldsymbol{Z}$ and $\boldsymbol{B}(k)$ are approximately known before clutter suppression. Thus, we can take the known $\boldsymbol{Z}$ and $\boldsymbol{B}(k)$ as prior information on the TDPC.

Assume that a target at the azimuth angle φ and elevation angle θ moves at a radial speed V_r related to the radar, and then the echo signal of the target at the slow time k can be described by [2]

$$s_{nk} = s_k(\varphi)\exp\{j(2\pi/\lambda)[nd\cos\theta\cos\varphi + (2kV_a/f_r)\cos\theta\cos(\varphi+\varphi_p) + 2kV_r/f_r]\} \quad (7)$$

where $s_k(\varphi)$ is the signal complex amplitude. Similarly, the target signal received by the N sensors and associated with the kth pulse can be written in the following matrix–vector form

$$\boldsymbol{s}(k) = s_k(\varphi)[\widehat{\omega}_k(\varphi)]\boldsymbol{z}(\varphi) = s_k(\varphi)[\widehat{\omega}(\varphi)]^k\boldsymbol{z}(\varphi) \quad (8)$$

where $\boldsymbol{z}(\varphi) = [z_1(\varphi), z_2(\varphi), \ldots, z_n(\varphi)]^T$ and $\widehat{\omega}_k(\varphi) = [\widehat{\omega}(\varphi)]^k$ in which $\widehat{\omega}(\varphi) = \exp\{j(2\pi/\lambda)[(2V_a/f_r)\cos\theta\cos(\varphi+\varphi_p) + 2V_r/f_r]\} = \omega(\varphi)\exp j[(2\pi/\lambda)(2V_r/f_r)]$. It is shown from a comparison of (5) with formula (8) that the temporal phase $(2\pi/\lambda)(2kV_r/f_r)$ caused by the Doppler frequency of the target makes the target signal different from the clutter signals.

3 Design of TDPC

To make the designed TDPC and relative algorithms workable, we assume that the ground clutter echoes satisfy the following often-used conditions [2]: (1) echo signals of two different ground-scatterer patches are statistically independent; (2) clutter echo signals are asymptotically Gaussian since the received ground clutter echoes are a sum of those by a large number of scatterers; (3) the fluctuations of ground clutter returns with the slow time are small enough so that the multiple returns of the same ground clutter patch are approximately equal during the CPI.

The above condition (3) implies $a_k(\varphi) = a_{k+1}(\varphi)$ or $\boldsymbol{a}_k = \boldsymbol{a}_{k+1}$, which can be satisfied by ignoring the internal clutter motion (ICM). Moreover, as shown in Section 2, the Doppler frequency causes a phase difference between the current and subsequent echoes scattered by the ground clutter and received by the antenna, which can be described by the diagonal matrix $\bar{\boldsymbol{B}}$. Thus, the ground clutter echoes

stimulated by the $k+1$th pulse and received by the antenna array can be written as

$$\begin{aligned} \boldsymbol{x}(k+1) &= \boldsymbol{Z}\boldsymbol{B}(k+1)\boldsymbol{a}_{k+1} + \boldsymbol{w}(k+1) \\ &= \boldsymbol{Z}\bar{\boldsymbol{B}}\boldsymbol{B}(k)\boldsymbol{a}_k + \boldsymbol{w}(k+1) \end{aligned} \tag{9}$$

On the basis of (5) and (9), an error function is defined as

$$\begin{aligned} \bar{\boldsymbol{\varepsilon}}(k) &= \boldsymbol{D}\boldsymbol{x}(k) - \boldsymbol{x}(k+1) = \boldsymbol{D}\boldsymbol{Z}\boldsymbol{B}(k)\boldsymbol{a}_k - \boldsymbol{Z}\bar{\boldsymbol{B}}\boldsymbol{B}(k)\boldsymbol{a}_k \\ &\quad + \boldsymbol{D}\boldsymbol{w}(k) - \boldsymbol{w}(k+1) \\ &= (\boldsymbol{D}\boldsymbol{Z} - \boldsymbol{Z}\bar{\boldsymbol{B}})\boldsymbol{B}(k)\boldsymbol{a}_k + \boldsymbol{D}\boldsymbol{w}(k) - \boldsymbol{w}(k-1) \\ &= \boldsymbol{\varepsilon}(k) + \boldsymbol{D}\boldsymbol{w}(k) - \boldsymbol{w}(k-1) \end{aligned} \tag{10}$$

where $\boldsymbol{D} \in C^{N\times N}$ denotes a coefficient matrix associated with the TDPC and $\boldsymbol{\varepsilon}(k) = (\boldsymbol{D}\boldsymbol{Z} - \boldsymbol{Z}\bar{\boldsymbol{B}})\boldsymbol{B}(k)\boldsymbol{a}_k$ is an error function associated with the ground clutter. The objective of the TDPC is to find an appropriate $\boldsymbol{D}$ such that $\|\boldsymbol{\varepsilon}(k)\|_F$ is minimised with subscript F denoting the Frobenius norm. Since $\boldsymbol{\varepsilon}(k)$ also depends on the unknown $\boldsymbol{a}_k$, its minimisation is not directly achieved. Fortunately, according to the Cauchy–Schwartz inequality, we have $\|\boldsymbol{\varepsilon}(k)\|_{\mathrm{F}} \le c\|\boldsymbol{D}\boldsymbol{Z} - \boldsymbol{Z}\bar{\boldsymbol{B}}\|_{\mathrm{F}}$, where an appropriate constant c is proportional to $\|\boldsymbol{B}(k)\boldsymbol{a}_k\|_{\mathrm{F}}$. Hence, $\min\|\boldsymbol{\varepsilon}(k)\|_{\mathrm{F}}^2$ can be achieved by $\min\|\boldsymbol{D}\boldsymbol{Z} - \boldsymbol{Z}\bar{\boldsymbol{B}}\|_{\mathrm{F}}^2$, since $\boldsymbol{Z}$ and $\bar{\boldsymbol{B}}$ can be determined by the parameters, position and moving speed of the airborne radar. Let the gradient of $\|\boldsymbol{D}\boldsymbol{Z} - \boldsymbol{Z}\bar{\boldsymbol{B}}\|_{\mathrm{F}}^2$ with respect to $\boldsymbol{D}$ be equal to zero, and then we easily obtain the following solution

$$\boldsymbol{D} = \boldsymbol{Z}\bar{\boldsymbol{B}}\boldsymbol{Z}^{\mathrm{H}}(\boldsymbol{Z}\boldsymbol{Z}^{\mathrm{H}})^{-1} \tag{11}$$

Since the cost function $\|\boldsymbol{D}\boldsymbol{Z} - \boldsymbol{Z}\bar{\boldsymbol{B}}\|_{\mathrm{F}}^2$ is quadratic, the above solution is unique and optimal.

Generate a data matrix $\boldsymbol{X} = \begin{bmatrix} \boldsymbol{x}(1), \ldots, \boldsymbol{x}(K-1) \\ \boldsymbol{x}(2), \ldots, \boldsymbol{x}(K) \end{bmatrix} \in C^{(2N)\times(K-1)}$ formed by all K data samples during the CPI, and then a TDPC pre-filtering operation for suppressing the ground clutter returns is given by

$$\boldsymbol{Y} = [\boldsymbol{D}|-\boldsymbol{I}]\boldsymbol{X} \tag{12}$$

where $\boldsymbol{Y} \in C^{N\times(K-1)}$ denotes the filtered output data matrix. Equation (12) describes a typical two-pulse canceller. If there are not any array error and speed error, most of the ground clutter should be suppressed by the TDPC.

Remark 1: It should be noted that since the drift angle φ_p and elevation angle θ have been taken into account in the design of the TDPC, the TDPC for suppressing the ground clutter is applicable not only to the sidelooking airborne radar but also to the non-sidelooking airborne radar. This is unlike the conventional DPCA processing that is applicable mainly in the sidelooking airborne radar because of the limitation of DPCA conditions. The relationship between the TDPC and DPCA is described in the Appendix.

Remark 2: The filter coefficient matrix $[\boldsymbol{D}|-\boldsymbol{I}]$ depends only on $\bar{\boldsymbol{B}}$ and $\boldsymbol{Z}$ that are determined by the velocity of the platform and the radar parameters. In addition, the parameters such as the platform velocity, the PRF and the transmission frequency will be changed by the radar operator, especially in pulse-Doppler radar systems, which may have multiple PRFs to stagger the insensitive area produced by the velocity ambiguities or/and range ambiguities. The TDPC coefficients should be changed with the change of the PRF, which is known for the signal processor. Thus, we can make a large look-up table of TDPC coefficients for every PRF, and the coefficients are required to filter out clutter in real-time processing. That can potentially reduce the computational burden in real-time processing.

Remark 3: The change in range and platform height leads to the change in the elevation angle and spatial phase matrix $\boldsymbol{Z}$. The TDPC pre-filter should be changed with the variation of the range and platform height. Fortunately, the same cancellation weights can be used in an appropriate range interval altered with the range, since the location of the clutter spectrum in the angle-Doppler space changes relatively slowly with the range [2]. Thus, we can recalculate a TDPC coefficient matrix within a range interval that is altered with the range, where a shorter interval and a longer interval should be taken at the near range and far range, respectively. Since the TDPC cancels the clutter in the angle-Doppler space, the TDPC is affected by the presence of range ambiguous clutter. Also, the TDPC is more sensitive to the near range ambiguous clutter and more insensitive to the far range ambiguous clutter.

4 TDPC pre-filtering approaches

We have exploited the prior information associated with the platform velocity and radar parameters to design TDPC. We expect such a TDPC to significantly eliminate the ground clutter returns in the space-time domain.

4.1 Conventional MTI with TDPC pre-filtering

To detect moving targets, the filtered space-time data are further processed by a match of signals in both spatial and temporal dimensions. The signal match along the spatial dimension is implemented by the following fixed beamforming

$$\boldsymbol{y}_b = \boldsymbol{z}^{\mathrm{H}}(\varphi)\boldsymbol{Y} = [\boldsymbol{z}^{\mathrm{H}}(\varphi)\boldsymbol{D}|-\boldsymbol{z}^{\mathrm{H}}(\varphi)]\boldsymbol{X} = \boldsymbol{b}\boldsymbol{X} \tag{13}$$

where $\boldsymbol{b} = [\boldsymbol{z}^{\mathrm{H}}(\varphi)\boldsymbol{D}|-\boldsymbol{z}^{\mathrm{H}}(\varphi)]$, $\boldsymbol{z}(\varphi)$ is the spatial steering vector directed at the target azimuth angle φ and elevation angle θ, and the row vector $\boldsymbol{y}_{\mathrm{b}} \in C^{1\times(K-1)}$ represents the output signal sequence. The match of signals along the

doi: 10.1049/iet-rsn:20080108

time direction is performed by a bank of Doppler filters

$$\boldsymbol{y}_{\mathrm{o}} = \boldsymbol{F}^{\mathrm{H}}\boldsymbol{y}_{\mathrm{b}}^{\mathrm{T}} \tag{14}$$

where $\boldsymbol{F}$ is a matrix in which all columns form a bank of FIR filters.

Once the output signal vector $\boldsymbol{y}_{\mathrm{o}}$ is obtained, all the elements of $\boldsymbol{y}_{\mathrm{o}}$ are fed into a detector. Thus, a processor for MTD consists of a ground clutter pre-filter $[\boldsymbol{D}|-\boldsymbol{I}]$, a fixed beamformer $\boldsymbol{z}(\varphi)$, a bank of Doppler filters $\boldsymbol{F}$ and a detector. Thus, the designed TDPC is a typical ground clutter pre-filter. In addition, it is worth pointing out that the so-called secondary sample data are not needed in the TDPC plus the conventional MTI method. Thus, the TDPC plus the conventional MTI method has a potential benefit that it is not affected by the problems of the limited sample support in the same manner as STAP techniques. This makes the TDPC suitable for heterogeneous clutter.

4.2 Dimension-reduced STAP with TDPC pre-filtering

The filtered data can be continuously processed by certain dimension-reduced STAP techniques [10–14] to further improve the performance of ground clutter suppression. The FA [10, 11] is widely recognised and commonly used as a developmental benchmark. Thus, the data filtered by the TDPC will be processed by the typical FA. The NK dimensional full adaptive problem is reduced to K different N-dimensional adaptive problems in the FA. This process is repeated for each of K Doppler bins.

Let the transformation matrix for the kth Doppler frequency bin be given by $\boldsymbol{T}_k = \boldsymbol{F}_k \otimes \boldsymbol{I}_N$, where $\otimes$ represents the Kronecker product of two matrices, $\boldsymbol{I}_N$ is the $N \times N$ identity matrix and $\boldsymbol{F}_k$ denotes a $K \times 1$ Doppler filter vector of the kth Doppler frequency bin. The space-time data vector $\boldsymbol{x}$ and space-time steering vector $\boldsymbol{s}$, respectively, are defined as $\boldsymbol{x} = [\boldsymbol{x}^{\mathrm{T}}(1), \boldsymbol{x}^{\mathrm{T}}(2), \ldots, \boldsymbol{x}^{\mathrm{T}}(K)]^{\mathrm{T}}$ and $\boldsymbol{s} = \boldsymbol{s}_{\mathrm{t}} \otimes \boldsymbol{s}_{\mathrm{s}}$, where $\boldsymbol{s}_{\mathrm{t}} \in C^{K\times 1}$ and $\boldsymbol{s}_{\mathrm{s}} \in C^{N\times 1}$ are the temporal steering vector and the spatial steering vector associated with the Doppler frequency and spatial phase shift across the array of the desired signal, respectively. Then the $N \times 1$ data vector and the space-time steering vector in the Fourier transform domain are therefore expressed as

$$\tilde{\boldsymbol{x}}_k = \boldsymbol{T}_k^{\mathrm{H}}\boldsymbol{x} \tag{15a}$$

$$\tilde{\boldsymbol{s}}_k = \boldsymbol{T}_k^{\mathrm{H}}\boldsymbol{s} \tag{15b}$$

It is well known that the adaptive weight vector for the mth Doppler frequency bin is given by

$$\tilde{\boldsymbol{w}} = \tilde{\boldsymbol{R}}_k^{-1}\tilde{\boldsymbol{s}}_k \tag{16}$$

where $\tilde{\boldsymbol{R}}_k$ is the $N \times N$ correlation matrix in Fourier transform domain and is expressible as

$$\tilde{\boldsymbol{R}}_k = E\{\tilde{\boldsymbol{x}}_k\tilde{\boldsymbol{x}}_k^{\mathrm{H}}\} = (\boldsymbol{F}_k \otimes \boldsymbol{I}_N)^{\mathrm{H}}\boldsymbol{R}(\boldsymbol{F}_k \otimes \boldsymbol{I}_N) \tag{17}$$

where $\boldsymbol{R} = E\{\boldsymbol{x}\boldsymbol{x}^{\mathrm{H}}\}$ is the correlation matrix of the ground clutter and noise signals.

Similar to (15a), the space-time data vector $\boldsymbol{x}$ is first pre-filtered by using the TDPC. The TDPC pre-filtering operation on the space-time data vector $\boldsymbol{x}$ and the space-time steering vector $\boldsymbol{s}$ is as follows

$$\breve{\boldsymbol{x}}_k = \boldsymbol{H}\boldsymbol{x} \tag{18a}$$

$$\breve{\boldsymbol{s}}_k = \boldsymbol{H}\boldsymbol{s} \tag{18b}$$

where the $N(K-1) \times NK$ filter matrix

$$\boldsymbol{H} = \begin{bmatrix} \boldsymbol{D} & -\boldsymbol{I} & \boldsymbol{0} & \boldsymbol{0} & \ldots & \boldsymbol{0} \\ \boldsymbol{0} & \boldsymbol{D} & -\boldsymbol{I} & \boldsymbol{0} & \ddots & \vdots \\ \boldsymbol{0} & \boldsymbol{0} & \ddots & \ddots & \ddots & \boldsymbol{0} \\ \vdots & \ddots & \ddots & \boldsymbol{D} & -\boldsymbol{I} & \boldsymbol{0} \\ \boldsymbol{0} & \ldots & \boldsymbol{0} & \boldsymbol{0} & \boldsymbol{D} & -\boldsymbol{I} \end{bmatrix} \in C^{[(K-1)N]\times(KN)} \tag{19}$$

The corresponding transformation matrix for the kth Doppler frequency bin is then given by

$$\breve{\boldsymbol{T}}_k = \breve{\boldsymbol{F}}_k \otimes \boldsymbol{I}_N \tag{20}$$

where $\breve{\boldsymbol{F}}_k$ is the $(K-1) \times 1$ Doppler filter vector for the kth Doppler frequency bin. If the space-time data vector $\boldsymbol{x}$ and space-time steering vector $\boldsymbol{s}$ in (15) are replaced by the filter data vector $\breve{\boldsymbol{x}}_k$ and filtered steering vector $\breve{\boldsymbol{s}}_k$, respectively, the FA after TDPC pre-filtering is similarly given by

$$\hat{\boldsymbol{x}}_k = \breve{\boldsymbol{T}}_k^{\mathrm{H}}\breve{\boldsymbol{x}} = \breve{\boldsymbol{T}}_k^{\mathrm{H}}\boldsymbol{H}\boldsymbol{x} \tag{21a}$$

$$\hat{\boldsymbol{s}}_k = \breve{\boldsymbol{T}}_k^{\mathrm{H}}\breve{\boldsymbol{s}} = \breve{\boldsymbol{T}}_k^{\mathrm{H}}\boldsymbol{H}\boldsymbol{s} \tag{21b}$$

$$\hat{\boldsymbol{w}} = \hat{\boldsymbol{R}}_k^{-1}\hat{\boldsymbol{s}}_k \tag{21c}$$

where $\hat{\boldsymbol{x}}_k$ and $\hat{\boldsymbol{s}}_k$ represent the new Fourier-transformed data and the Fourier-transformed steering vector for the FA with TDPC pre-filtering, respectively; $\hat{\boldsymbol{w}}$ denotes the adaptive weight vector for the FA with TDPC pre-filtering; and $\hat{\boldsymbol{R}}_k$ is the estimated correlation matrix in the new Fourier transform domain and is expressible as

$$\hat{\boldsymbol{R}}_k = E\{\hat{\boldsymbol{x}}_k\hat{\boldsymbol{x}}_k^{\mathrm{H}}\} = \breve{\boldsymbol{T}}_k^{\mathrm{H}}\boldsymbol{H}\boldsymbol{R}\boldsymbol{H}^{\mathrm{H}}\breve{\boldsymbol{T}}_k \tag{22}$$

Hence, we derive the new FA with TDPC pre-filtering.

It can be seen from (21) and (22) that the TDPC pre-filtering approach has spatial-temporal dimension-reduced

processing steps. The first dimension-reduced step implemented by $\boldsymbol{H}$ is mainly used as ground clutter cancellation. The second dimension-reduced step is implemented by the dimension-reduced matrix $\boldsymbol{T}_k$. Therefore we expect that the FA with TDPC pre-filtering can improve the MTD performance, compared with the FA.

Finally, we analyse the computational complexity of the proposed algorithms in real-time processing. The TDPC coefficients have been calculated offline and required for real-time processing. To conveniently determine the computational complexity of the proposed algorithms, we assume that the same TDPC coefficient matrix is used to process L neighbourhood range gates, where L also represents the number of the sampling data. The Doppler filtering is implemented by DFT. The multiplication and division number is marked the MDN for short, which is used as an index of the computational complexity. It should be first noted that the MDN for computing $\boldsymbol{b} = [\boldsymbol{z}^{\mathrm{H}}(\varphi)\boldsymbol{D}|-\boldsymbol{z}^{\mathrm{H}}(\varphi)]$ is N^2, the MDN for computing $\boldsymbol{bX}$ is $2(K-1)N^2L$ and the MDN for computing $\boldsymbol{y}_o = \boldsymbol{F}^{\mathrm{H}}\boldsymbol{y}_{\mathrm{b}}^{\mathrm{T}}$ is $2(K-1)KL$. Thus, the MDN for the conventional MTI and the MDN for the conventional MTI with TDPC pre-filtering are about $KN^2L + K^2L$ and $N^2 + 2(K-1)N^2L + (K-1)KL$, respectively. Furthermore, the MDN for the FA and the MDN for the FA with TDPC pre-filtering are approximately $NK^2L + KN^2L + 2KN^3/3 + N^2K + NKL$ and $N^2(K-1)L + NK(K-1)L + KN^2L + 2KN^3/3 + N^2K + NKL$, respectively. Moreover, the MDN for the EFA with three temporal DOFs and the MDN for the EFA with TDPC pre-filtering are about $NK^2L + K(3N)^2L + 2K(3N)^3/3 + (3N)^2K + 3NKL$ and $N^2(K-1)\ L + NK(K-1)L + K(3N)^2L + 2K(3N)^3/3 + (3N)^2K + 3NKL$, respectively. The computational complexity of the conventional MTI with pre-filtering is much smaller than that of the FA and the EFA. Also, it can be also seen by comparing the pre-filtering approaches with the original methods that the additional computational load increased by the TDPC pre-filtering operation is relatively small.

5 Experimental results

To illustrate the performance gains caused by the TDPC, we conduct two numerical experiments that use the simulated data and measured data. The improvement factor (IF) is defined as the ratio of the output SCNR to the input SCNR. The system performance of a processor can be well exhibited by IF. The performances of six algorithms, the conventional MTI, the TDPC plus the conventional MTI, the FA, the TDPC plus the FA, the EFA and the TDPC plus the EFA will be shown via experimental results.

5.1 Detection performance using simulated radar data

This experiment uses simulated data based on a 32×32 rectangular antenna array mounted on an aircraft. The ground clutter is modelled as the sum of the contributions of many discrete far-field sources [13]. Here, we uniformly place 300 discrete sources, where the angle between two adjacent sources is 0.6°. The amplitude of each source is a complex Gaussian random variable and has been weighted by the transmit beam pattern of the array. The noise is Gaussian white noise whose average power is equal to 1 so that the ground clutter and target signal powers are referenced to the white-noise power. The mainbeam has −35 dB Chebyshev weights. Let the variance of both the amplitude and phase error of the array-element be 2%. Assume that the azimuth angle of the mainbeam is $\varphi_0 = 90°$ and that the elevation angle of the mainbeam is 0°. Let $\lambda = 0.2\,\mathrm{m}$, $d = \lambda/2$, $f_{\mathrm{r}} = 2800\,\mathrm{Hz}$, $V_{\mathrm{a}} = 140\,\mathrm{m/s}$ and $H = 13.5\,\mathrm{Km}$. The size of the range gate is 150 m since the pulsewidth is set to be 1 μs. The maximum clutter range is $R_{\max} = 400\,\mathrm{km}$. The number of range ambiguity is $N_{\mathrm{c}} = \mathrm{INT}[(R_{\max} - H)/R_{\mathrm{u}}] = 7$, where $R_{\mathrm{u}} = c/(2f_{\mathrm{r}})$ is the ambiguity range, c is the velocity of light, and INT[β] denotes that β is rounded to the nearest integer. Each of 32 column subarrays is synthesised first, and the ratio of clutter to noise (CNR) at the column-subarray level is the CNR = 60 dB. The test range gate is located at 250 Km. To show the performance of the TDPC, a moving target with an SNR of 0 dB is injected into the test range cell. The target is situated at $\varphi = 90°$ and has the Doppler frequency $f_{\mathrm{d}} = 0.25f_{\mathrm{r}}$. The TDPC weights are derived using synthetic clutter for a single unambiguous range ring of clutter and can be applied to simulated range ambiguous clutter data in the experiments.

Fig. 1*a* shows the minimum variance distortionless response (MVDR) spectra of the received data within the range bin in the presence of a target for sidelooking radar systems ($\varphi_P = 0°$). The ground clutter ridge with slope 1 is clearly seen in the Doppler frequency and spatial frequency space. Fig. 1*b* shows the MVDR spectra of the data filtered by the TDPC for the target range bin. The ground clutter ridge is considerably suppressed by the TDPC and there is just a little residual ground clutter in the mainlobe region. It can also be seen that the target signal is not significantly corrupted by the TDPC. In this regard, the target can be easily detected from the filtered data, if the target signal is matched along both spatial and temporal dimensions as shown in (13) and (14).

The performances of six relative algorithms are shown in Fig. 2, where Figs. 2*a* and 2*b* are for the sidelooking radar ($\varphi_P = 0°$) and non-sidelooking radar ($\varphi_P = -30°$), respectively. As shown in Fig. 2, the performance of the conventional MTI with the TDPC pre-filter is worse than that of the two tap pre-Doppler STAP, whereas the performance of the FA with the TDPC pre-filter is better than that of the two tap pre-Doppler STAP. It can be seen from Fig. 2*a* that the performance of the approaches with TDPC pre-filtering is much better than that of the approaches without TDPC pre-filtering for the sidelooking radar. Especially, the approaches with TDPC pre-filtering can effectively improve the performance in the Doppler

IET Radar Sonar Navig., 2009, Vol. 3, Iss. 2, pp. 133–143
doi: 10.1049/iet-rsn:20080108

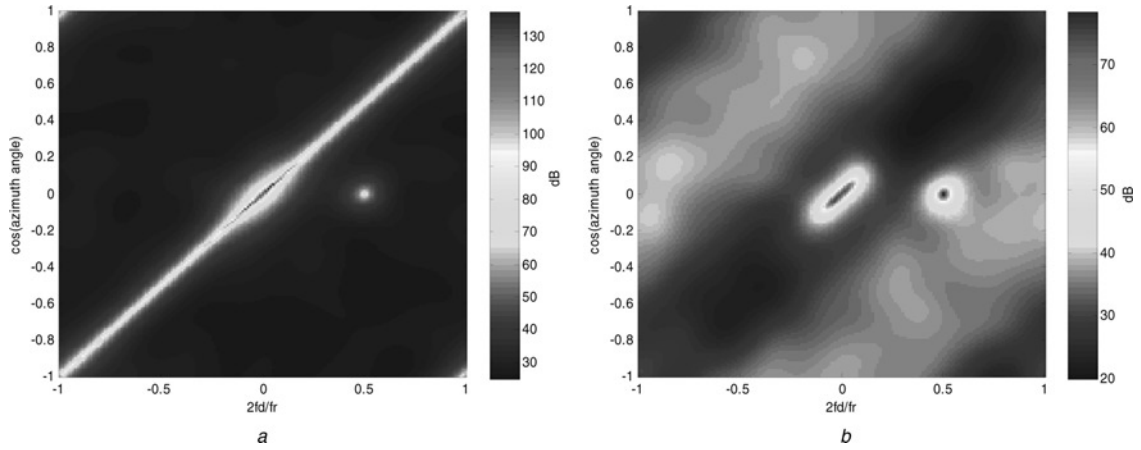

Figure 1 *Comparison of the MVDR spectra of the original data with the filtered data*

a MVDR spectra of the original data
b MVDR spectra of the filtered data

frequency region near the mainlobe clutter. Hence, the approaches with TDPC pre-filtering have a stronger capability of detecting the slowly moving targets. Good performance gains can also be achieved by the TDPC for the non-sidelooking radar as shown in Fig. 2*b*. It should be noted that these performance gains are achieved mainly by pre-filtering the ground clutter implemented by the TDPC. The ground clutter cancellation before the conventional MTI or the FA and the EFA implies that there is a lower interference level in the filtered data, facilitating performance improvement.

5.2 Detection performance using measured radar data

To illustrate the good ground clutter rejection capability of the TDPC, a performance evaluation is given by using measured data from a database of multichannel airborne radar measurements [27]. These experiments use data from acquisition 575 on flight 5 (file rl050575). In these experiments, the main parameters for calculating the TDPC are as follows: the platform velocity is $V_a = 100.2$ m/s, the drift angle $\varphi_p = 7.28^\circ$, the array element spacing $d = 0.1092$ m, the radar wavelength $\lambda = 0.2419$ m, the PRF $f_r = 1984$ Hz and the elevation angle $\theta = 4^\circ$.

Fig. 3 shows the results obtained by the conventional MTI and the TDPC plus the conventional MTI. To make the performance evaluation convincing, one strong artificial target with an SCNR of -20 dB is injected at the range bin 405 and three weak artificial targets with an SCNR of -40 dB are injected at the range bins 410, 420 and 425, where ground clutter and noise power is averaged by the five-bin average, centred on the test range bin where the target is placed. All targets have the same azimuth angle $\varphi = 90^\circ$ and Doppler frequency $f_d = -0.148 f_r$. All the 11 azimuth channels and the 128 pulses are used for the match of signals. It can be seen from Fig. 3 that strong

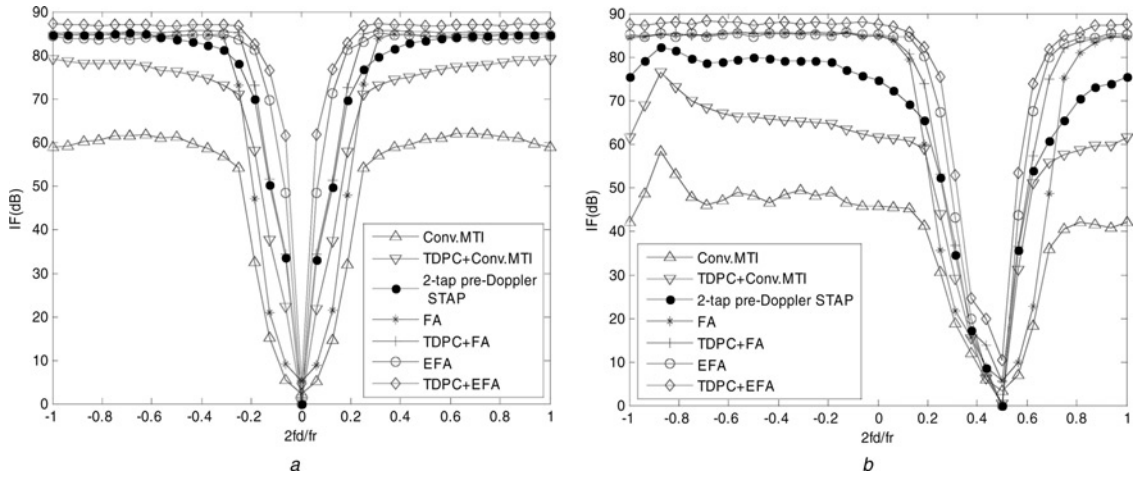

Figure 2 *Curves of IF against* $2f_d/f_r$

a $\varphi_P = 0^\circ$
b $\varphi_P = -30^\circ$

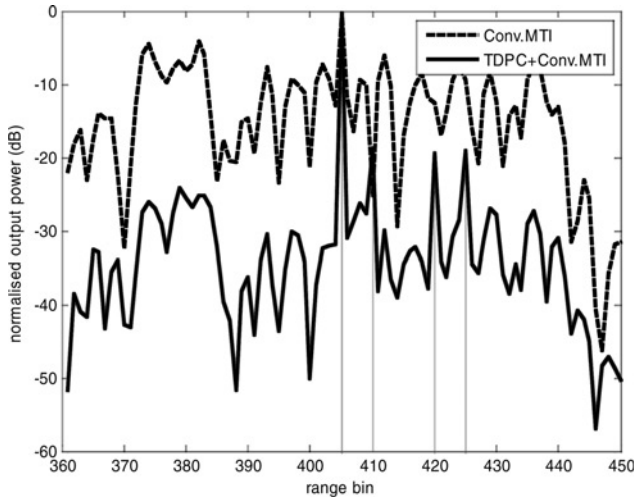

Figure 3 *Curves of normalised output power against range bin for the conventional MTI with and without TDPC pre-filtering*

residual ground clutter left by the conventional MTI submerges the three weak target signals, and that only the strongest target at the range bin 405 is brought out with only 10.8 dB above the mean value. The TDPC plus the conventional MTI makes all the targets clearly seen since a ground clutter cancellation of about 21.2 dB is achieved by TDPC pre-filtering. The three weak targets are brought out with at least 12.2 dB above the mean value. It should be noted that this performance gain is also mainly obtained by the ground-clutter pre-filtering operation implemented by the TDPC.

Fig. 4 illustrates the performance gain obtained by using the TDPC pre-filter before the FA and the EFA. In these experiments, all the 11 azimuth channels and the first 32 pulses are used for pre-filtering and the FA and EFA. All the correlation matrices of the ground clutter and noise are estimated using the range bins from 360 to 450, neglecting the test cell and its two neighbourhood cells. The two weak artificial targets with an SCNR of −36 dB, an azimuth angle of 90° and a Doppler frequency of $-0.148f_r$ were injected at the range bins 420 and 425. It can be seen from Fig. 4*a* that the power of the targets relative to the average residual clutter power is 15.2 dB for the FA and 22.8 dB for the TDPC plus the FA. The FA with pre-filtering has an improvement of 7.6 dB compared with the FA. As shown in Fig. 4*b*, the EFA brings out the two weak targets with 24.4 dB above the mean value, whereas the EFA with TDPC pre-filtering extracts the weakest target with at least 27.2 dB above the mean value. This is an improvement of 2.8 dB over the EFA without pre-filtering. These results illustrate that the proposed algorithms achieve relatively good performance at the improvement of an output SCNR and the corresponding detection probability under a constant probability of false alarm.

6 Conclusions

In this paper, we have proposed a TDPC pre-filter for airborne radar ground clutter suppression. The TDPC is essentially a space-time clutter canceller that filters out the clutter in the space-time domain. The clutter model and moving target model are first formulated in the matrix–vector form. The location of the clutter spectrum in the angle-Doppler space is determined by the platform velocity, platform height, range and radar parameters including the wavelength, PRF and array manifold. This prior information has been exploited for designing the TDPC.

The design of the TDPC has been explained on the basis of the ground clutter model in a matrix-vector form. Like the DPCA technique, the TDPC is also a space-time clutter suppressor. Since the drift angle and elevation angle have been considered in the design of the TDPC, the TDPC can

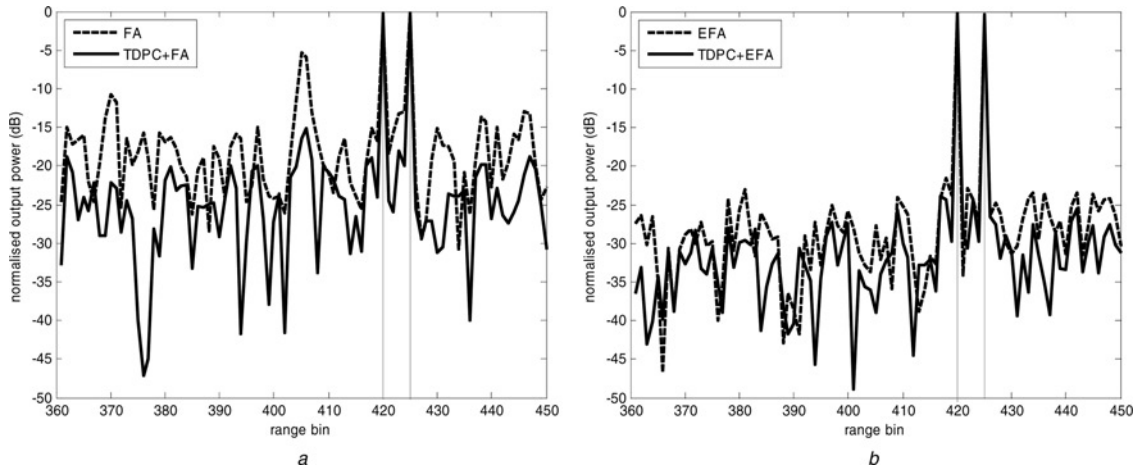

Figure 4 *Curves of normalised output power against range bin for the FA with and without TDPC pre-filtering and the EFA with and without TDPC pre-filtering*

a Results obtained by the FA with and without TDPC pre-filtering
b Results obtained by the EFA with and without TDPC pre-filtering

IET Radar Sonar Navig., 2009, Vol. 3, Iss. 2, pp. 133–143
doi: 10.1049/iet-rsn:20080108

effectively suppress clutter for both the sidelooking and non-sidelooking airborne radars. This is unlike the DPCA technique which is usually used in the sidelooking airborne radar and limited by the DPCA conditions. The TDPC can be implemented via a large look-up table of coefficients, which are calculated in offline processing, which leads to a low computational load for real-time processing.

Finally, the use of the TDPC pre-filter before the conventional MTI processing and the two dimension-reduced STAP techniques have been proposed. The TDPC plus the conventional MTI processing is robust to non-homogeneous clutter since it is not limited by the problem of sample support in the same manner as the STAP techniques. Besides, the TDPC can efficiently reduce the clutter level and it is helpful to further improve the performance of the dimension-reduced STAP algorithm. Numerical experiments using both simulated and measured data have been presented to illustrate the satisfactory performance of the TDPC pre-filter in comparison with the conventional MTI, FA and EFA.

7 References

[1] GUERCI J.R.: 'Space-time adaptive processing for radar' (Artech House, Norwood, MA, 2003)

[2] KLEMM R.: 'Space-time adaptive processing; principles and applications'. IEE Radar Sonar Navigation and Avionics, 1998, vol. 9

[3] WARD J.: 'Space-time adaptive processing for airborne radar'. Technical Report ESC-TR-94-109, Lincoln Laboratory, December 1994

[4] MELVIN W.L.: 'A STAP overview', *IEEE Trans. Aerosp. Electron. Syst. Mag.*, 2004, **19**, (1), pp. 19–35

[5] SEBASTIEN D.G., PHILIPPE R., FABIAN D.L., JACQUES G.V.: 'Framework and taxonomy for radar space-time adaptive processing (STAP) methods', *IEEE Trans. Aerosp. Electron. Syst.*, 2007, **43**, (3), pp. 1084–1099

[6] WICKS M.C., RANGASWAMY M., ADVE R., HALE T.B.: 'Space-time adaptive processing', *IEEE Signal Process. Mag.*, 2006, pp. 51–65

[7] PECKHAM C.D., HAIMOVICH A.M., AYOUB T.F., GOLDSTEIN J.S., REED I.S.: 'Reduced-rank STAP performance analysis', *IEEE Trans. Aerosp. Electron. Syst.*, 2000, **36**, (2), pp. 664–676

[8] GUERCI J.R., GOLDSTEIN J.S., REED I.S.: 'Optimal and adaptive reduced-rank STAP', *IEEE Trans. Aerosp. Electron. Syst.*, 2000, **36**, (2), pp. 647–663

[9] SKOLNIK I.M.: 'Radar handbook' (McGraw-Hill, New York, 1990)

[10] DIPPETRO R.C.: 'Extended factored space-time processing for airborne radar system'. Proc. 26th Asilomar Conf. Signals, Systems and Computers, October 1992, pp. 425–430

[11] BAO Z., LIAO G.S., WU R.B., ZHANG Y.H., WANG Y.L.: 'Adaptive spatial-temporal processing for airborne radars', *Chin. J. Electron.*, 1993, **2**, (1), pp. 2–7

[12] BAO Z., WU S., LIAO G.S., XU Z.Y.: 'Review of reduced rank space-time adaptive processing for airborne radar'. Proc. Int. Conf. Radar, Beijing, China, 1996, pp. 766–769

[13] WANG H., CAI L.: 'On adaptive spatial-temporal processing for airborne surveillance radar systems', *IEEE Trans. Aerosp. Electron. Syst.*, 1994, **30**, (3), pp. 660–669

[14] ADVE R.S., HALE T.B., WICKS M.C.: 'Joint domain localized adaptive processing in homogeneous and non-homogeneous environments, part I: homogeneous environments', *IEE Proc., Radar Sonar Navig.*, 2000, **147**, pp. 66–73

[15] BROWN R.D., SCHNEIBLE R.A., WICKS M.X., WANG H., ZHANG Y.: 'STAP for clutter suppression with sum and difference beams', *IEEE Trans. Aerosp. Electron. Syst.*, 2000, **36**, (2), pp. 634–646

[16] GOLDSTEIN J.S., REED I.S., ZULCH P.A.: 'Multistage partially adaptive STAP CFAR detection algorithm', *IEEE Trans. Aerosp. Electron. Syst.*, 1999, **35**, (2), pp. 645–661

[17] ROMAN J.R., RANGASWAMY M., DAVIS D.W., ZHANG Q., HIMED B., MICHELS J.H.: 'Parametric adaptive matched filter for airborne radar applications', *IEEE Trans. Aerosp. Electron. Syst.*, 2000, **36**, (2), pp. 677–692

[18] RANGASWAMY M., MICHELS J.H., HIMED B.: 'Statistical analysis of the non-homogeneity detector for STAP applications', *Digit. Signal Process.*, 2004, **14**, (3), pp. 253–267

[19] RANGASWAMY M.: 'Statistical analysis of the non-homogeneity detector for non-Gaussian interference backgrounds', *IEEE Trans. Signal Process.*, 2005, **53**, (6), pp. 2101–2111

[20] WANG Y.L., CHEN J.W., BAO Z., PENG Y.N.: 'Robust space-time adaptive processing or airborne radar in nonhomogeneous clutter environments', *IEEE Trans. Aerosp. Electron. Syst.*, 2003, **39**, (1), pp. 70–81

[21] CPARARO C., CAPRARO G., WEINER D., WICKS M.: 'Improved STAP performance using knowledge-aided secondary data selection'. Proc. 2004 IEEE Radar Conf., Philadelphia, PA, April 2004, pp. 361–365

[22] CAPRARO C.T., CAPRARO G.T., DE MAIO A., FARINA A., WICKS M.: 'Demonstration of knowledge-aided space-time adaptive processing using measured airborne data', *IEE Proc., Radar Sonar Navig.*, 2006, **153**, (6), pp. 487–494

[23] CHRISTOPHER T.C., GERARD T.C., IVAN B., DONALD D.W., MICHAEL C.W., WILIAM J.B.: 'Implementing digital terrain data in knowledge-aided space-time adaptive processing', *IEEE Trans. Aerosp. Electron. Syst.*, 2006, **42**, (3), pp. 1080–1099

[24] SHANNON D.B., KARL G., RANGASWAMY M.: 'STAP using knowledge-aided correlation estimation and the FRACTA algorithm', *IEEE Trans. Aerosp. Electron. Syst.*, 2006, **42**, (3), pp. 1043–1057

[25] MELVIN W.L., SHOWMAN G.A.: 'An approach to knowledge-aided covariance estimation', *IEEE Trans. Aerosp. Electron. Syst.*, 2006, **42**, (3), pp. 1021–1042

[26] FARINA A., LOMBARDO P., CARAMANICA F.: 'Non-linear non-adaptive clutter cancellation for airborne early warning radar'. IEE Int. Radar Conf., Radar'97, Edinburgh, October 1997, pp. 420–424

[27] SLOPER D., FENNER D., ARNTZ J., FOGLE E.: 'Multi-channel airborne radar measurement (MCARM), MCARM fight test', Westinghouse electronic systems, Contract F30602-92-C-0161, April 1996, Available: http://sunrise.deepthought.rl.af.mil

8 Appendix: relationship of TDPC and DPCA

The special notations used in this appendix are given here. A $K \times K$ identify matrix is denoted as $\boldsymbol{I}_K$. A $K \times K$ zero matrix is denoted as $\boldsymbol{0}_K$. A $K \times 1$ zero vector $\boldsymbol{0}_{K\times 1}$ and $1 \times K$ zero vector $\boldsymbol{0}_{1\times K}$ imply $\boldsymbol{0}_{K\times 1} = [0, 0, \ldots, 0]^{\mathrm{T}} \in C^{K\times 1}$ and $\boldsymbol{0}_{1\times K} = [0, 0, \ldots, 0] \in C^{1\times K}$, respectively. Give the $K \times L$ matrix $\boldsymbol{\Phi} = (\phi_{m,n}) \in C^{K\times L}$ with $m = 1, \ldots, K$ and $n = 1, \ldots, L$, then an operator $[\boldsymbol{\Phi}]_{(K_1:K_2,L_1:L_2)} = (\phi_{m,n}) \in C^{(K_2-K_1+1)\times(L_2-L_1+1)}$ with $m = K_1, \ldots, K_2$ and $n = L_1, \ldots, L_2$, where $K_1 \le K_2 \le K$ and $n = L_1 \le L_2 \le L$. Thus, $[\boldsymbol{\Phi}]_{(K_1:K_2,L_1:L_2)} = (\phi_{m,n})$ is a submatrix of $\boldsymbol{\Phi}$.

When the DPCA conditions $d = 2V_{\mathrm{a}}T$ are satisfied and $\varphi_p = 0^\circ$, we can obtain

$$(2\pi/\lambda)(2V_{\mathrm{a}}/f_{\mathrm{r}})\cos\theta\cos(\varphi+\varphi_p) = (2\pi/\lambda)d\cos\theta\cos\varphi = \Phi \tag{23}$$

$$z_n(\varphi) = \exp[j(2\pi/\lambda)nd\cos\theta\cos\varphi] = \exp(jn\Phi) \tag{24}$$

$$\omega_k(\varphi) = \exp[j(2\pi/\lambda)(2V_{\mathrm{a}}/f_{\mathrm{r}})k\cos\theta\cos(\varphi+\varphi_p)] = \exp(jk\Phi) \tag{25}$$

Define the temporal and spatial-temporal phase terms of the clutter echo from a point scatter at the angle φ_i as $z_n(\varphi_i) = \exp(jn\Phi_i)$ and $\omega_k(\varphi_i) = \exp(jk\Phi_i)$, respectively. Let $\boldsymbol{A} = \boldsymbol{Z}\boldsymbol{B}\boldsymbol{Z}^{\mathrm{H}}$, and $\bar{\boldsymbol{A}} = \boldsymbol{Z}\boldsymbol{Z}^{\mathrm{H}}$, then $\boldsymbol{D} = \boldsymbol{A}\bar{\boldsymbol{A}}^{-1}$. It is directly deduced that

$$\boldsymbol{A} = \begin{pmatrix} \sum_{i=I}^{I}\exp(j\Phi_i) & I \\ \sum_{i=I}^{I}\exp(j2\Phi_i) & \sum_{i=I}^{I}\exp(j\Phi_i) \\ \vdots & \vdots \\ \sum_{i=I}^{I}\exp(j(N-1)\Phi_i) & \sum_{i=I}^{I}\exp(j(N-2)\Phi_i) \\ \sum_{i=I}^{I}\exp(jN\Phi_i) & \sum_{i=I}^{I}\exp(j(N-1)\Phi_i) \end{pmatrix} \begin{pmatrix} \sum_{i=I}^{I}\exp(-j\Phi_i) & \cdots & \sum_{i=I}^{I}\exp(-j(N-2)\Phi_i) \\ I & \cdots & \sum_{i=I}^{I}\exp(-j(N-3)\Phi_i) \\ \ddots & \ddots & \vdots \\ \cdots & \sum_{i=I}^{I}\exp(j\Phi_i) & I \\ \cdots & \sum_{i=I}^{I}\exp(j2\Phi_i) & \sum_{i=I}^{I}\exp(j\Phi_i) \end{pmatrix} \tag{26}$$

$$\bar{\boldsymbol{A}} = \begin{pmatrix} I & \sum_{i=I}^{I}\exp(-j\Phi_i) \\ \sum_{i=I}^{I}\exp(j\Phi_i) & I \\ \vdots & \vdots \\ \sum_{i=I}^{I}\exp(j(N-2)\Phi_i) & \sum_{i=I}^{I}\exp(j(N-3)\Phi_i) \\ \sum_{i=I}^{I}\exp(j(N-1)\Phi_i) & \sum_{i=I}^{I}\exp(j(N-2)\Phi_i) \end{pmatrix} \begin{pmatrix} \sum_{i=I}^{I}\exp(-j2\Phi_i) & \cdots & \sum_{i=I}^{I}\exp(-j(N-1)\Phi_i) \\ \sum_{i=I}^{I}\exp(-j\Phi_i) & \cdots & \sum_{i=I}^{I}\exp(-j(N-2)\Phi_i) \\ \ddots & \ddots & \vdots \\ \cdots & I & \sum_{i=I}^{I}\exp(-j\Phi_i) \\ \cdots & \sum_{i=I}^{I}\exp(j\Phi_i) & I \end{pmatrix} \tag{27}$$

It can be seen from (26) and (27) that $[\boldsymbol{A}]_{(2:N,1:N)} = [\bar{\boldsymbol{A}}]_{(1:N-1,1:N)}$, and

$$\boldsymbol{A} = \begin{pmatrix} \boldsymbol{0}_{(N-1)\times 1} & \boldsymbol{I}_{N-1} \\ 0 & \boldsymbol{0}_{1\times(N-1)} \end{pmatrix}\bar{\boldsymbol{A}} + \begin{pmatrix} [\boldsymbol{0}_N]_{(1:N-1,1:N)} \\ [\boldsymbol{A}]_{(N:N,1:N)} \end{pmatrix} \tag{28}$$

doi: 10.1049/iet-rsn:20080108

Hence, the coefficients matrix $\boldsymbol{D}$ is expressible as

$$\boldsymbol{D} = \begin{pmatrix} \mathbf{0}_{(N-1)\times 1} & \boldsymbol{I}_{N-1} \\ 0 & \mathbf{0}_{1\times(N-1)} \end{pmatrix} + \begin{pmatrix} [\mathbf{0}]_{(1:N-1,1:N)} \\ [\boldsymbol{A}]_{(N:N,1:N)} \end{pmatrix} \bar{\boldsymbol{A}}^{-1} = \begin{pmatrix} \mathbf{0}_{(N-1)\times 1} & \boldsymbol{I}_{N-1} \\ [\bar{\boldsymbol{a}}]_{(1:1,1:1)} & [\bar{\boldsymbol{a}}]_{(1:1,2:N)} \end{pmatrix} \tag{29}$$

where $\bar{\boldsymbol{a}} = [\boldsymbol{A}]_{(N:N,1:N)}\bar{\boldsymbol{A}}^{-1}$. The TDPC $[\boldsymbol{D}|-\boldsymbol{I}] \in C^{N\times(2N)}$ used to filter out clutter is written as

$$\boldsymbol{Y} = [\boldsymbol{D}|-\boldsymbol{I}]\begin{pmatrix} \boldsymbol{x}_k \\ \boldsymbol{x}_{k+1} \end{pmatrix} = \begin{pmatrix} [\boldsymbol{x}_k]_{(2:N,1:1)} - [\boldsymbol{x}_{k+1}]_{(1:N-1,1:1)} \\ \bar{\boldsymbol{a}}\boldsymbol{x}_k - [\boldsymbol{x}_{k+1}]_{(N:N,1:1)} \end{pmatrix} \tag{30}$$

Like the classic DPCA technique, $[\boldsymbol{x}_k]_{(2:N,1:1)} - [\boldsymbol{x}_{k+1}]_{(1:N-1,1:1)}$ in the TDPC indicates that the clutter signal received by the first $N-1$ array at the $k+1$ th instant of time is cancelled by using clutter received by the last $N-1$ array at the k th instant of time. However, $\bar{\boldsymbol{a}}\boldsymbol{x}_k - [\boldsymbol{x}_{k+1}]_{(N:N,1:1)}$ in the TDPC indicates the clutter echo received by the N th element of the array at the $k+1$ th instant of time is suppressed by interpolation and an echo-subtraction scheme, and this operation is absent in the DPCA technique. Hence, the DPCA method would be a special case of the TDPC method when the DPCA condition is satisfied, and the performance of the TDPC is slightly better than that of the DPCA technique since the $\bar{\boldsymbol{a}}\boldsymbol{x}_k - [\boldsymbol{x}_{k+1}]_{(N:N,1:1)}$ is involved in the TDPC.

Besides, we would like to point out that the TDPC can still work by interpolation and an echo-subtraction scheme when the DPCA condition is not satisfied. Thus, the TDPC is a more general technique for clutter suppression.